# Several phosphate transport processes are present in vascular smooth muscle cells

Luis Hortells, Natalia Guillén, Cecilia Sosa, Víctor Sorribas

Department of Toxicology, Veterinary Faculty, University of Zaragoza, Zaragoza, Spain

**Running head title:** Pi transport in vascular cells

**Address for Correspondence**

Victor Sorribas

University of Zaragoza. Veterinary Faculty. Department of Toxicology

Calle Miguel Servet 177

Zaragoza, 50013, Spain

Tel: +34 976761631

Fax: +34 976761612

E-mail: sorribas@unizar.es

**Author contributions**:

LH performed most of the experiments, analyzed data, and helped with text preparation.

NG performed experiments, analyzed data, and helped with text preparation.

CS performed experiments, analyzed data, and helped with text preparation.

VS designed the work, analyzed results, and prepared the manuscript and figures.

**ORCID codes:**

LH: 0000-0003-1923-4918

NG: 0000-0001-6627-298X

CS: 0000-0003-2907-0427

VS: 0000-0003-3457-323X

**Abstract**

We have studied Pi handling in rat aortic vascular smooth muscle cells (VSMC) using $^{32}$P-radiotracer assays. Our results have revealed a complex set of mechanisms consisting in 1) well-known PiT1/PiT2-mediated sodium-dependent Pi transport; 2) Slc20-unrelated sodium-dependent Pi transport that is sensitive to the stilbene derivatives 4,4'-diisothiocyanatostilbene-2,2'-disulphonic acid (DIDS) and (4-acetamido-4-isothiocyanostilbene-2,2-disulfonate) (SITS); 3) a sodium-independent Pi uptake system that is competitively inhibited by sulfate, bicarbonate, and arsenate and is weakly inhibited by DIDS, SITS, and phosphonoformate; and 4) an exit pathway from the cell that is partially chloride-dependent and unrelated to the known anion-exchangers expressed in VSMC. The inhibitions of sodium-independent Pi transport by sulfate and of sodium-dependent transport by SITS were studied in greater detail. The maximal inhibition by sulfate was similar to that of Pi itself, with a very high inhibition constant (212 mM). SITS only partially inhibited sodium-dependent Pi transport, but the $K_i$ was very low (14 μM). Nevertheless, SITS and DIDS did not inhibit Pi transport in *Xenopus laevis* oocytes expressing PiT1 or PiT2. Both the sodium-dependent and sodium-independent transport systems were highly dependent on VSMC confluence and on the differentiation state, but they were not modified by incubating VSMC for 7 days with 2 mM Pi under non-precipitating conditions. This work not only shows that the Pi handling by cells is highly complex, but also that the transport systems are shared with other ions such as bicarbonate or sulfate.

**Keywords**: phosphate transport; vascular cells; sodium independent; anion exchanger

**New & Noteworthy**

In addition to PiT1 and PiT2, rat vascular smooth muscle cells show a sodium-dependent Pi transport system that is inhibited by DIDS and SITS. A sodium-independent Pi uptake system of high affinity is also expressed, which is inhibited by sulfate, bicarbonate, and arsenate. The exit of excess Pi is through an exchange with extracellular chloride. Whereas the metabolic effects of the inhibitors, if any, cannot be discarded, kinetic analysis during initial velocity suggests competitive inhibition.

## Introduction

Cells use inorganic phosphate (Pi) for many critical functions, including energy storage and transfer, signal transduction, the post-translational modification of proteins, cytosolic buffering, nucleic acid and biomembrane compositions, etc. To guarantee an adequate supply of Pi, cells need specific sodium-coupled Pi transporters in the plasma membrane to overcome the hydrophobicity, the negative charges, and the uphill chemical gradient of the Pi anions (4, 14). The polyprotic characteristic of Pi means that, under physiological conditions, Pi anions are only significantly present as monovalent ($H_2PO_4^-$, monobasic) or divalent ($HPO_4^=$, dibasic) phosphates, and at physiological pH (7.4), divalent Pi is more than twice the concentration of monovalent Pi. The difference in the negative charges mandates the selectivity of the different Pi transporters: the Slc34 family (which includes the type II Pi transporters NaPiIIa, NaPiIIb, and NaPiIIc) has a preference for the divalent anion (4,13,14), while the Slc20 members (which include type III, PiT1, and PiT2) preferentially transport the monobasic, $H_2PO_4^-$ (4, 14, 24). The Slc34 family of Pi transporters is mainly (but not exclusively) responsible for the control of Pi homeostasis due to the uphill uptake of divalent Pi (the most abundant) in intestinal and renal epithelia. The role of Slc20 transporters in the control of Pi homeostasis is unclear, but as a consequence of general cell expression, these transporters seem to play a critical role in supplying Pi to cells (29). This is at first surprising because these transporters preferentially carry the less abundant Pi ($H_2PO_4^-$), but even so Pi transport is saturated in cells such as VSMC (32), despite the fact that type III Pi transporters seemed to be the only sodium-dependent Pi transporters expressed in VSMC (11). The frequent simultaneous expression of PiT1 and PiT2 in the same cell constitutes an apparent redundancy, which led to the

suspicion (and later proof) that these transporters have functions other than merely Pi transport, such as cell proliferation, apoptosis, signaling, etc. (5, 10, 17, 26, 29).

Vascular smooth muscle cell (VSMC) cultures show sodium-dependent Pi uptake that seems to be completely mediated by PiT1 and PiT2 (21, 32). In addition, an inward sodium-independent Pi transport system has been functionally described in VSMC (32), but the molecular identity is still unknown. This sodium-independent transport system should be coupled to another, direct or indirect source of energy to compensate for the membrane potential (negative inside). Finally, cells also express an efflux system for the exit of excess Pi, and whereas the functional characteristics of this Pi efflux diverge among cell types, the only efflux system to be identified thus far is XPR1, a retroviral receptor of xenotropic and polytropic murine leukemia retroviruses (16). The exit of excess Pi from VSMC has not been characterized, and the expression of XPR1 protein is unknown.

It has been suggested that both VSMC Pi transport and the Slc20 Pi transporters play a critical role in the pathogenesis of vascular calcification (11, 15), although this proposal has turned out to be scientifically controversial (33, 36). The *in vitro* model of calcification used to study the role of Pi transport in vascular calcification was shown to be unrelated to vascular calcification, rather it was related to unsuspected experimental calcium precipitation (19). Therefore, Pi transport in VSMC still needs to be characterized, for physiological and pathological reasons. In this work we have conducted a more in-depth study of the characteristics of Pi transport in the aortic VSMC of rat, the aim of which is to better understand the physiology of the arterial wall and the pathogenesis of the progression of medial vascular calcification.

## Materials and Methods

### *Vascular Smooth Muscle Cells*

The VSMC used in the present study correspond to the same isolation batch described previously, from the aorta of 2-month old rats (19). Cells were cultured in Minimum Essential Medium (Lonza, Basel, Switzerland), with additional glutamine, antibiotics, and 10% fetal calf serum, in 5% $CO_2$.

### *Transport assays and analyses*

Pi transport assays were performed under initial velocity conditions (10 minutes in VSMC, 1 hour in *Xenopus* oocytes), using orthophosphoric acid-$^{32}$P (PerkinElmer, Waltham, MA, USA), as described (17). Pi uptake or accumulation is expressed as nmol Pi per milligram of cell protein and per minute, in both VSMC and oocytes, in the *Xenopus* heterologous expression system. Pi transport saturation experiments were also performed for kinetic analysis (see below).

For the studies with different pH values, MES (4-morpholineethanesulfonate) and Tris (2-amino-2-(hydroxymethyl)-1,3-propanediol) were used, both from Sigma-Aldrich (St Louis, MO, USA). For the experiments with inhibitors, bicarbonate was added before use, and the pH was adjusted again with Tris-HCl. For oxalate, both control and oxalate-containing transport media were prepared without calcium. For the short incubation time that was used (10 minutes, initial velocity), the absence of calcium did not affect Pi transport, the total cell protein per well, the number of cells, or the cell morphology (see Results).

For the experiments in which the role of chloride was studied, all salts in the uptake medium that contained chloride were replaced with the corresponding gluconate salts (all from Sigma). The Tris buffer was also pH-adjusted using gluconic acid. To study the exit

of Pi from VSMC, these cells were loaded with $^{32}$Pi (0.05 mM Pi) for three hours in uptake solution, then they were washed and incubated in uptake medium without Pi for the indicated times. The total $^{32}$P (phosphorus) of the uptake (hereafter, "exit") medium was quantified by scintillation at several different times and was calculated as the exit of grams of phosphorus per milligram of VSMC protein. Both the total (accumulated) and the net P content in uptake medium per well were calculated, as well as the total P per unit of time (efflux rate). The progression of P accumulated in medium was studied with regression lines, whereas for both the net exit and the P accumulated in medium per minute, exponential decay curves were obtained using non-linear regression fits. In all cases, a replicates test was performed to determine whether or not the model was adequate.

To determine the kinetic parameters of both Pi saturation and transport inhibition, non-linear regressions was performed as described (30) using GraphPad Prism for Macintosh (GraphPad Software, La Jolla, CA, USA). The determinations of the half inhibition concentration ($IC_{50}$) were performed by sigmoidal dose-response fits to the data. And for the affinity constant ($K_i$) calculations, global shared parameter fits to the following competitive equation were carried out:

$$V = \frac{V_{max} \times S}{K_{mObs} + S} + K_d \times S;\ K_{mObs} = K_m \times \frac{1 + [I]}{K_i}$$

Where $K_{mObs}$ is the affinity observed in the presence of the inhibitor, and $K_d$ is the diffusion constant or slope of the unsaturated uptake, which includes the unspecific binding of $^{32}$P.

146 *mRNA expression analysis*

147 For non-quantitative RNA expression, RNA was purified using a ChargeSwitch Total RNA
148 Cell Kit (Thermo-Fisher, Massachusetts, USA), and it was reverse-transcribed using the
149 SuperScript III First-Strand Synthesis System for RT-PCR (Thermo-Fisher).

150 For Real Time PCR, retrotranscription was performed using a PrimeScript RT Reagent Kit
151 (Perfect Real Time, Takara Bio Inc., Kusatsu, Japan), with SYBR Premix Ex Taq II
152 (Takara) in a LightCycler 1.5 (Roche, Mannheim, Germany). The sequences of primers are
153 listed in table 1. The results were normalized to GAPDH and to a calibrator, following the
154 manufacturer's instructions.

155 *Immunoblotting*

156 VSMC were lysed in RIPA buffer (0.01 M Tris-Cl pH 7.4, 0.14 M NaCl, 1% deoxycholate,
157 0.1% sodium dodecyl sulfate, 1% Triton X-100, 1x protease inhibitors; all components
158 from Sigma), and the lysate was centrifuged at 5,000 g. The supernatant protein was
159 quantified by the bicinchoninic acid method (Pierce BCA Protein Assay kit, Thermo-
160 Fisher). Western-blots were performed as described (9) with the following commercial
161 antibodies: anti-calponin 1 (sc-16604-R), anti-MGP (sc-66965), and anti-Sm22α (sc-
162 18513), all three of which were from Santa Cruz Biotechnology (Heidelberg, Germany);
163 anti-α-Smooth Muscle Actin (A5228) and anti ß-actin (A1978) antibodies were from
164 Sigma Aldrich; and anti-PiT1 and anti-PiT2 were polyclonal antibodies reported previously
165 (9). The signals of the specific bands were optimized with several dilutions of the primary
166 and secondary antibodies. Expressions were quantified in relation to ß-actin signals, which
167 were not modified in these studies.

*Interference of RNA transcripts*

For knocking down specific RNA expression, short-interfering RNAs (siRNA) were designed and obtained as Silencer Select siRNAs from Life Technologies-Ambion (Austin, TX, USA). They were transfected with Lipofectamine 2000 (Life Technologies) as described (8), and the effect on function was observed 48 hours later.

*Xenopus oocytes*

*Xenopus laevis* oocytes were obtained from the European Xenopus Resource Centre, curated with funding from the Welcome Trust/BBSRC and maintained by the University of Portsmouth, School of Biological Sciences (UK). Oocytes were defolliculated, injected, and incubated as described (32). The cloning and expression of rat PiT1 have been described before (32). For PiT2, kidney cortex RNA was reverse-transcribed using the SuperScript III First-Strand Synthesis System for RT-PCR, and the complete cDNA of rat PiT2 was amplified with Platinum™ Taq DNA Polymerase High Fidelity (Thermo-Fisher) and the following primers: sense, TCCATCGCTTTCCAGAGCAG; antisense, TGGCTGAGTTCTAAGCTCGC. The cDNAs were cloned with a TOPO TA cloning kit, were *in vitro*-transcribed with a Message Machine Transcription kit (Invitrogen), and were polyadenylated with a Poly (A) Tailing kit (both from ThermoFisher Scientific).

*Statistics*

All experiments were repeated at least three times, and at least triplicates were used in each experiment. The exact number of replicates is indicated in the legends. The results are shown as a mean + standard error. Analysis of Variance was used to compare more than 2 means, and the Tukey post-test was used for multiple comparisons. For the comparison of

two means, a t-test was used. For the statistical differences of either the linear or non-linear regression fits, F tests were performed to provide p values on the corresponding null-hypotheses and to determine the best fit. To check for the linearity of regression, a runs test was performed to determine the number of runs and if the residuals of the series of points were either positive or negative. To establish if the model (equation) used in the non-linear regression was adequate for the experimental data, a replicates test was used, which analyzes the scattering of data as a Gaussian random variation around the selected model. The goodness-of-fit of the linear and non-linear regressions was also determined with the $r^2$, which measures the relationship between X and Y by determining the fraction of the variation that is shared between X and Y. GraphPad Prism software was also used for all statistical analyses.

## Results

### *Kinetic characteristics of Pi transport*

The first experiments were performed basically to characterize Pi transport and to confirm that the kinetic behavior of Pi transport in our VSMC had not changed with respect to previous studies (32). Pi transport saturation experiments confirmed the existence of inward Pi transport, in either the presence or absence of sodium, with apparent affinities of 0.15 and 0.16 mM Pi, respectively (Figs. 1A and B). In this experiment, the $V_{max}$ in the presence of sodium was 5 times higher than the $V_{max}$ in the absence of sodium, as shown in Fig. 1B, after elimination of the unsaturable component.

Another hallmark of Pi transport in VSMC is the pH-dependence of uptake in the presence of sodium. Uptake is highest at acidic pH, and it decreases when pH increases (Fig. 1C). This is most likely related to the expression of the type III Pi transporters, PiT1 and PiT2, because the preferred substrate (monovalent Pi) is most abundant at acidic pH. In the absence of sodium, however, we did not observe that pH had any significant effect on Pi uptake.

### *Effect of tissue culture confluence on Pi transport and differentiation*

Pi uptake was also studied as a function of the confluence of VSMC in culture. Studies at approximately 5, 10, 50, and 100% confluence revealed no effect on total Pi uptake per milligram of protein in the presence of sodium (Fig. 2A). Sodium-independent Pi uptake, however, decreased progressively, reaching a minimum at 100% confluence. Total Pi uptake was therefore maintained due to an increase of the net, sodium-dependent Pi uptake, depending on the extent of VSMC confluence.

To determine if the effect of confluence on Pi transport was due to VSMC differentiation, the expression of several genes related to the smooth muscle phenotype was also analyzed

by comparing the expression at 50 vs. 100% confluence. Both RNA and the protein abundance of the Pi transporter PiT1 increased with confluence, which could explain the increase in sodium-dependent Pi transport observed in Fig 2A. However, the expressions of both PiT2 RNA (with respect to GAPDH) and protein (with respect to ß-actin) were not modified (Figs. 2B and 2C). In both cases – PiT1 and PiT2 – we have only compared the total amount of protein, but reorganization in homodimers or heterodimers, as in the case of the response to changes in the Pi concentration of the culture media in osteoblastic and chondrocytic cells, cannot be ruled out (6).

Smooth muscle markers, such as calponin (RNA only), Sm22α, and α-Smooth muscle actin, also showed increased RNA expression with confluence. By contrast, the expression of the calcification inhibitor, matrix Gla protein (MGP), was reduced for both RNA and protein (Figs. 2B and C).

*Effect of chloride on Pi uptake*

In addition to the sodium dependence of VSMC Pi transport, we also sought to study chloride dependence. To study the effect on sodium-dependent Pi uptake, sodium chloride was equimolarly replaced by sodium D-gluconate. Given that we were unable to obtain or easily produce choline gluconate, in this experiment N-methyl-D-glucamine chloride was used as a sodium-independent condition, and the effect of chloride was studied using N-methyl-D-glucamine D-gluconate. The other chloride-containing salts of the uptake media were also replaced by the corresponding gluconate-containing salts.

Figure 3A shows that the absence of chloride caused an increase in Pi accumulation in both the presence and absence of sodium. The increase was approximately 50% in both cases, with slight differences among the triplicated experiments. Because both sodium-activated and sodium-independent Pi uptakes are mediated by different transport systems, a

simultaneous inhibitory effect by chloride on these two uptake systems is unlikely. Rather, the effect of chloride withdrawal – an increase in Pi content – was most probably caused by the inhibition of an efflux pathway of Pi from the cell. To confirm this, and also to decrease the probability of a stimulatory effect by gluconate, VSMC were first incubated for 3 hours (arbitrary time) with 0.05 mM $^{32}$Pi to load the cells. The net uptake after this accumulation was greater in the absence of chloride ($P < 0.05$) than when it was present (69.5 and 36.5 nanograms P per milligram of protein, respectively) (Fig. 3B). The reason why the accumulated $^{32}$P is expressed as grams of phosphorus rather than as moles of Pi is because after 3 hours Pi can be metabolized and incorporated into other macromolecules, and therefore the molecular entity is unknown. The cells were then washed several times and incubated in uptake medium without Pi, in the presence or absence of chloride. The remaining $^{32}$P content in the cell (meaning 7.4 ng P/mg protein) was not significantly different among the various conditions used, but in the condition characterized by the absence of chloride the P content was always slightly higher (Fig. 3B). $^{32}$P in media was determined and expressed per mg of cell protein at every time point (Fig. 3C), thereby revealing an increased exit over time in the presence of chloride, with a regression line slope of $0.2287 \pm 0.0769$ and an $r^2$ of 0.1890. Conversely, in the absence of chloride, P accumulation in medium was half the concentration observed with chloride, and the slope ($0.0758 \pm 0.0915$) was not significantly different from zero ($r^2$ of 0.0177). Both regression lines were not identical ($P < 0.0001$), and in both cases the linearity model was adequate. In addition, in the presence of chloride the slope was different from zero ($p = 0.0051$), whereas in the absence of chloride the slope was not ($p = 0.4129$).

When the accumulation in medium was divided per time to determine the rate at every time interval, the efflux dropped exponentially (Fig. 3D). Non-linear regressions were performed

using an exponential equation, thereby providing half-time parameters for P accumulation in medium of 23.5 minutes in the presence of chloride and 16.7 minutes in the absence of chloride. When instead of total phosphorus in medium, the net phosphorus per time point was calculated, a steeper exponential drop was observed (Fig. 3D, inset), with half-life values of 7 and 5 minutes, respectively. Despite the fact that the half-life in the absence of chloride was smaller than with chloride, the P content in medium was always smaller when no chloride was present at all time points, even when some single points did not have significant differences. Also, very importantly, most of the P exit in VSMC takes place very quickly, and it is similar to the entrance rate.

*Inhibition profile of Pi transport*

In order to more precisely characterize the Pi handling in VSMC, either as Pi influx or efflux, we analyzed the inhibition profile using a series of substrates and inhibitors of anion exchangers (Fig. 4). Sodium-dependent Pi transport was completely inhibited using Pi itself as the inhibitor (5 mM). Arsenate (10 mM) and the anion exchangers 4,4'-diisothiocyanatostilbene-2,2'-disulphonic acid (DIDS) and (4-acetamido-4-isothiocyanostilbene-2,2-disulfonate) (SITS) (0.1 mM each) inhibited sodium-dependent Pi transport by 70-75%. The effects of 10 mM sulfate, 10 mM bicarbonate, 5 mM phosphonoformate (PFA), and 10 mM oxalate were not significant (Fig. 4A). To avoid oxalate precipitation, a calcium-free uptake medium was used. The absence of calcium for 10 minutes did not affect Pi transport, total cell protein (13.62±0.53 vs. 13.86±0.45 $\mu g/cm^2$ for cells incubated with and without calcium), or cell morphology (Fig. 4B).

Sodium-independent Pi transport was more sensitive to the assayed inhibitors (Fig. 4C). Maximal inhibition was obtained with phosphate and sulfate, bicarbonate and arsenate,

while the inhibitions with PFA, SITS and DIDS were less intense. Once again, oxalate did not affect Pi transport.

Because sodium-dependent Pi transport in VSMC seems to be mediated mostly by PiT1 and PiT2, these transporters were expressed in oocytes and assayed for the inhibitory effect of DIDS and SITS. As shown in Fig. 4C, these stilbene derivatives, used at 0.1 mM, did not affect the Pi transport of rat PiT1 or PiT2 when they were heterologously expressed in *Xenopus laevis* oocytes. Furthermore, no effects were observed when the oocytes were preincubated with DIDS or SITS for 30 minutes, or even longer, before the phosphate was added (not shown).

The weak inhibition of sodium-independent Pi transport by sulfate, bicarbonate, or arsenate was further analyzed in VSMC using dose-response relationship studies at a constant 0.05 mM Pi (Fig. 5). The results confirmed the first findings and revealed that complete inhibition was not even reached at the highest concentrations of inhibitors used (50 mM). This impeded an accurate determination of the inhibition parameters, with a preliminary half inhibition concentration ($IC_{50}$) of 21, 36, and 27 mM for sulfate, bicarbonate, and arsenate, respectively. The $K_i$ constants for the three inhibitors were therefore not calculated using these $IC_{50}$ values.

Dose-response assays were also performed on VSMC with DIDS and SITS in the presence of sodium (Fig. 5). In these cases, the inhibitions were also incomplete at the maximal concentrations of inhibitors used, therefore impeding any accurate kinetic analyses. With this limitation, the half inhibition concentrations were estimated, showing that the $IC_{50}$ of SITS (8.2 μM) was 18 times lower than the $IC_{50}$ of DIDS (178 μM) at the concentration of 0.05 mM Pi.

Several inhibition constants were calculated by performing Michaelis-Menten saturation assays in the presence of different but fixed concentrations of the inhibitors (and therefore, variable concentrations of Pi for each inhibition concentration). Figure 6 shows the assays for sulfate in the absence of sodium and for SITS in the presence of sodium. In both cases, Lineweaver-Burk linear transformations suggested that both inhibitions were competitive. To determine the $K_i$ values, non-linear regressions using global shared parameters were performed as described (30), thereby confirming the weak inhibition of sulfate, with a $K_i$ value of 212 mM, which was 14 μM for SITS.

*Role of bicarbonate transporters and anion exchangers*

Even if the effects of the stilbene derivatives on sodium-independent Pi transport were low, this finding, in combination with the effects of sulfate and bicarbonate, suggested the likely involvement of a member of the Slc4 or Slc26 families of bicarbonate and anion exchangers. Consequently, using reverse transcription and non-quantitative PCR, first the RNA expressions of Slc4a2, Slc4a3, Slc4a7, Slc26a2, Slc26a6, Slc26a8, Slc26a10, and Slc26a11 in confluent VSMC were determined (not shown). Then the expression of these transporters was studied quantitatively by real time PCR using RNA obtained from VSMC at either 50% or 100% confluence for correlation with the changes observed in Pi uptake (Fig. 7A). A *t*-test was used to compare the significance of the specific expressions, and it revealed that the expressions of Slc4a3, Slc26a2, Slc26a6, and Slc26a8 increased significantly with confluence. If these transporters played a role in the efflux of Pi, then an increased expression with confluence could explain the reduced uptake in the absence of sodium observed in confluent VSMC (Fig. 2A).

To clarify whether or not these transporters (Slc4a2, Slc4a3, Slc4a7, Slc26a2, Slc26a6, Slc26a8, Slc26a10, and Slc26a11) played any role in sodium-independent uptake or in the

efflux of Pi from the cells, specific knocking-down of the RNAs was performed using siRNA transfections. The expressions of the corresponding RNA transcripts were reduced to at least 70-80% (Fig. 7B). After 48 hours, the uptake of Pi revealed that none of the interfered transporters were responsible for a significant part of the sodium-independent influx or efflux of Pi in VSMC (Fig. 7C).

*Effect of a chronically high Pi concentration on the uptake and exit of Pi in VSMC*

Finally, we determined whether the exit of P from the cell could be modulated by incubating the VSMC in a high-Pi medium, thereby mimicking hyperphosphatemic concentrations. To avoid alkaline calcium supersaturation and homogeneous precipitation, cells were incubated in DMEM-F12 medium and 5% $CO_2$ with either 1 or 2 mM (non-radioactive) Pi (19). After 7 days under these conditions, we measured the sodium-dependent and sodium-independent Pi uptake at initial velocity with 0.05 mM $^{32}$Pi, i.e., only Pi entry into the cell (10 min). No effect of incubation with 2 mM Pi for 7 days was observed in either the sodium-dependent or sodium-independent Pi uptake compared to the uptakes in VSMC incubated with 1 mM Pi (Fig. 8A).

To check the effect on P exit from the cell after incubation for 7 days at 1 or 2 mM Pi, cells were washed and incubated in uptake medium with $^{32}$Pi as described in Methods and in Fig. 3B. The results are shown in Fig. 8B, revealing that after 7 days of incubation with a high or normal Pi concentration, the P exiting from cells in the incubation medium also did not change.

## Discussion

In this work we have studied Pi transport and handling in VSMC for several reasons, including the fact that these cells constitute a good *in vitro* model for studying non-epithelial Pi transport and because they have been used as a model for studying the role of Pi transport in vascular calcification.

Regarding the fact that VSMC constitute a good *in vitro* model for studying non-epithelial Pi transport, we have shown that these cells exhibit several components of transport (summarized in Fig. 9) that are not usually and simultaneously found in other cell lines: a sodium-dependent Pi uptake system, a sodium-independent influx system, and an efflux system that is needed to eliminate the excess of intracellular Pi. Each one of these transport systems seems to have more than one component. For example, two inward transporters from the Slc20 family, namely PiT1 and PiT2, are components of the sodium-dependent Pi transport system in VSMC. However, the specific reduction of expression, or even the deletion, of these transporters does not completely nullify sodium-dependent Pi transport (11, 32), consequently suggesting the presence of additional transport systems, which concurs with the conclusions of this work. Furthermore, PiT1 and PiT2 show additional functions and subcellular organelle expression other than Pi transport and plasma membrane, respectively (5-7, 10, 26, 33). When PiT1 RNA is interfered, for example in the Opossum Kidney proximal tubular cell line, Pi transport is not affected, but when siRNA is directed to the much less abundant PiT2, the inhibition of expression dramatically reduces Pi uptake (17). In this case, PiT2 could have functions other than Pi transport, such as being a Pi sensor (6), a role that is compatible with the expression of an intracellular sensor of Pi (34) according to the expression location of these transporters (33).

Sodium-dependent Pi transport in VSMC responds to pH changes similar to pH effects on PiT1- and PiT2-mediated transport, which suggests a preference for monovalent Pi (Fig. 1) (32). Sodium-dependent Pi transport in VSMC shows high affinity to Pi, and resistance to phosphonoformic acid (PFA; Fig. 4A), similarly to the two SLC20 transporters (24, 32, 35). Inhibition with PFA only occurs at a very high concentration, whereas members of the Slc34 family of Pi transporters are inhibited at a much lower concentration (30, 31). Most importantly, we have observed that sodium-dependent Pi transport in VSMC is partially sensitive to the stilbene derivatives, DIDS and SITS (at the same level as arsenate inhibition; Fig. 4A), whereas PiT1- and PiT2-mediated transport is completely resistant to DIDS and SITS (Fig. 4C). The inhibition is competitive, and SITS shows a very high affinity ($K_i$ of SITS is 14.4 μM; Fig. 6). The maximal inhibition reached in VSMC with DIDS and SITS is not very high (Fig. 5), and this agrees with the presence of the sodium-dependent, stilbene-resistant SLC20 Pi transporters. To our knowledge, this is the first description of DIDS/SITS-sensitive Pi transport.

With respect to sodium-independent uptake, the relevance (capacity or $V_{max}$) with respect to total transport ranges from 16.2% in the present study to 46% in a previous work (32). The difference can be explained not only by the different passages of VSMC but also by the differentiation stage of the cells, as shown in Fig. 2, because sodium-independent transport decreases with differentiation in culture. This transport also shows a high affinity for Pi (approximately 0.1 mM), similar to the sodium-dependent component (Fig. 1 and ref. 10). It is important to point out that this transport is not affected by pH, and it therefore most likely handles monovalent and divalent phosphate similarly. Even if this transport system is sodium-independent, it is most likely not equilibrative, but rather coupled to some source of

energy because the electrochemical gradient of Pi impedes the free entry of Pi into the cell. Therefore, the negative charges of Pi should be neutralized by the cotransport of cations or, most likely, by the exit of anions. This is why the sodium-dependent carriers of divalent Pi, Slc34a1 (NaPiIIa) and 2 (NaPiIIb), show a stoichiometry of 3:1 for $Na^+$:$Pi^=$. In Slc34a3 (NaPiIIc) it is 2:1, and the monovalent Pi carriers, PiT1 and PiT2, function with a stoichiometry of 2:1 for $Na^+$:$Pi^-$. Therefore, all transporters are rheogenic except for NaPiIIc, which carries divalent Pi in combination with only two sodium ions (27).

Regarding the inhibition pattern of sodium-independent Pi transport, it was inhibited by more compounds than sodium-dependent Pi transport (Fig. 4A). PFA, DIDS and SITS are very weak inhibitors; and sulfate, bicarbonate, arsenate and phosphate reached the maximal inhibition. As it was previously stated regarding SITS and DIDS, the low inhibitions are partially explained by the presence of a multitude of Pi transporters in these cells. However, in the case of sulfate, even if competitive (Fig. 6), the high $K_i$ (4,000 times the apparent affinity of Pi) rules out any of the known sodium-independent sulfate transporters as candidates for Pi transporters. This was confirmed through the expression analysis of known sulfate transporters (Fig. 7). The conclusion from all the aforementioned is that a high-affinity, sodium-independent Pi transporter is present in these cells, with a high specificity for Pi uptake.

The characterizations of the inhibitions in this study were performed using short incubation times, corresponding to the initial velocity, i.e., when the entrance of $^{32}P$ is equivalent to the net uptake (meaning a non-significant exit can be observed). Also, the kinetic analyses of the inhibitions revealed competitive inhibitions. These two facts suggest that inhibitions act directly on transporters rather than indirectly due to mechanisms related to metabolism,

pharmacology, or pH changes. Nevertheless, this will only be clarified after the corresponding transporters are identified.

A similar sodium-independent transport system has been described in capillaries of the blood-brain barrier (12). The authors used additional substrates as inhibitors, showing similar but not identical results because the concentrations and the data analyses were very different. However, the system was sodium- and energy-independent, saturable, and of high affinity (0.16 mM Pi), and it was also inhibited by sulfate, arsenate, PFA, DIDS, and SITS. Pi uptake is slightly *trans*-stimulated with bicarbonate, a mechanism that is inhibited with DIDS, and it is chloride-independent. This transport system (12) shows important differences with respect to the system that we have described in VSMC, such as strong inhibition with only 1 mM sulfate and the role played by chloride.

Other sodium-independent uptake systems that have been described in detail are present in the basolateral membrane of the renal proximal tubules (2) and in articular chondrocytes (28). A basolateral Pi uptake system in the proximal tubules would supply Pi to the cells when the reabsorption rate is minimal. The system's calculated affinity is, however, extremely low ($K_m$ 10 mM Pi). Moreover, the system is *trans*-stimulated with Pi, is resistant to sulfate and PFA, and is therefore unrelated to the sodium-independent uptake system in VSMC. In articular chondrocytes, sodium-independent uptake was inhibited by phosphonoacetate and arsenate, and it was not affected by pH changes (28). Finally, we have also described two sodium-independent Pi transport systems in the intestinal Caco2BBE cell line, depending on the concentration of Pi in the culture medium (8). Both transporters show a very high affinity for Pi and respond differently to not only inhibitors but also to changes in pH. The transport observed in these cells incubated with 1 mM Pi is

very similar to the transport observed in VSMC, with some differences such as the response to alkaline pH, which inhibits Pi uptake in Caco2BBE.

We have also described a chloride-dependent exit of P from the cell (Fig. 3). Our results are preliminary and were only designed to help identify the missing transporters. Several candidates from the Slc4 and Slc26 families exchange chloride with several common anions, such as bicarbonate or sulfate (1,25). Most of the Slc4 transporters and some of the Slc26 family are DIDS-sensitive. If this were the case in VSMC, we would observe an increased accumulation of Pi in the cells with stilbene-derivative compounds, yet conversely, we see an inhibition (Figs. 4 and 5). Also, the main candidates of these families are ruled out either due to the absence of expression of some transporters or the non-effect of specific RNA interference (Fig. 7C), despite the increased expression of some of these transporters with confluence (Fig. 7A). Few studies have reported on the exit of Pi from the cell, with most of them mainly focused on the basolateral membrane of the proximal tubular cells. One work described the sodium-independent exit of Pi, non-sensitive to DIDS and electroneutral, most likely in exchange with hydroxyl anions (22). Another exchange of Pi was described several years later in Opossum Kidney (OK) cells (3), which was compatible with the low affinity uptake of Pi described previously as an exchange (2). In this case, two intracellular molecules of monovalent Pi could be exchanged with one molecule of extracellular divalent Pi or citrate, therefore being electroneutral but also independent of chloride. It is important to point out that we have not characterized the composition of the Pi that exits from the cells. Considering that VSMC were incubated for 3 hours with 50 μM $^{32}$Pi, the $^{32}$phosphorus could be incorporated into nucleotides, phospholipids, phosphorylated proteins, polyphosphates, etc. In the case of pyrophosphate

(PPi), for example, the intracellularly synthesized calcification inhibitor most likely exits the cell through the ANK membrane protein (18) that is expressed in VSMC (23), and therefore some of the $^{32}$P that exits the cell will not be $^{32}$Pi but $^{32}$PPi. ANK functions independently of chloride, and therefore the likely exit of PPi is an explanation for the $^{32}$P that exits the cell independently of chloride (Fig. 3), in addition to other Pi-containing compounds.

Finally, after it was proposed that increased Pi transport was necessary for the pathogenesis of ectopic vascular calcification (11, 15), we showed that such an increase was barely observed under hyperphosphatemic conditions because uptake in VSMC is already saturated at physiological concentrations of Pi. Therefore, no additional Pi will enter cells by merely increasing the concentration of Pi in uptake media or in blood plasma, unless more Pi transporters are expressed (33, 36). In this work we analyzed the modulation of Pi efflux by incubating cells for a week with 2 mM Pi and using pH-controlled media to avoid calcium supersaturation and precipitation (19). Neither the uptake (Fig. 8A) nor the exit (Fig. 8B) of Pi were regulated/modulated by or adapted to a high Pi concentration for 7 days. Again, our results do not support the proposal that Pi transport is involved in the pathogenesis of vascular calcification, but they do agree with our previous work showing initial calcium deposits well before hyperphosphatemia is observed in an experimental model of chronic kidney disease, therefore also suggesting that this ectopic calcification is independent of Pi transport (20).

In conclusion, despite the in-depth knowledge that has been gained over the last 25 years regarding the control of Pi homeostasis and the sodium-dependent handling of Pi, much is still unknown. Regarding VSMC alone, several Pi transport systems still need to be

identified: an additional sodium-dependent Pi transporter that is sensitive to DIDS and SITS and that uses monovalent Pi; a sodium-independent Pi transporter of high affinity that handles monovalent and divalent Pi; and a sodium-independent efflux system that is chloride-dependent. The literature shows the existence of even more unknown Pi transport systems, representing a significant challenge that still needs to be addressed.

**Acknowledgments**

Present address of LH**:** The Heart Institute, Division of Molecular Cardiovascular Biology, Cincinnati Children's Hospital Medical Center, Cincinnati, OH, USA.

**Grants**

This work was supported by two grants from the Ministry of Economy and Competitiveness, code SAF2015-66705-P, PGC2018-098635-B-I00, and a grant from the "Gobierno de Aragón" and from FSE, "Construyendo Europa desde Aragón", code B39_17R, all three to V.S.

**Disclosures**

The authors have no conflicts of interest to declare.

## References


1. **Alper SL, Sharma AK.** The SLC26 gene family of anion transporters and channels. *Mol Aspects Med.* 34: 494-515, 2013.
2. **Azzarolo AM, Ritchie G, Quamme GA**. Some characteristics of sodium-independent phosphate transport across renal basolateral membranes. *Biochim Biophys Acta.*1064: 229-234, 1991.
3. **Barac-Nieto M, Alfred M, Spitzer A**. Basolateral phosphate transport in renal proximal tubule-like OK cells. *Exp Biol Med (Maywood)* 227:626-631, 2002.
4. **Biber J, Hernando N, Forster I**. Phosphate transporters and their function. *Annu Rev Physiol*. 75: 535-550, 2013.
5. **Bon N, Frangi G, Sourice S, Guicheux J, Beck-Cormier S, Beck L**. Phosphate-dependent FGF23 secretion is modulated by PiT2/Slc20a2. *Mol Metab.* 11: 197-204, 2018
6. **Bon N, Couasnay G, Bourgine A, Sourice S, Beck-Cormier S, Guicheux J, Beck L**. Phosphate (Pi)-regulated heterodimerization of the high-affinity sodium-dependent Pi transporters PiT1/Slc20a1 and PiT2/Slc20a2 underlies extracellular Pi sensing independently of Pi uptake. *J Biol Chem*. 293: 2102-2114, 2018.
7. **Byskov K, Jensen N, Kongsfelt IB, Wielsøe M, Pedersen LE, Haldrup C, Pedersen L**. Regulation of cell proliferation and cell density by the inorganic phosphate transporter PiT1. *Cell Div.* 7: 7, 2012.
8. **Candeal E, Caldas YA, Guillén N, Levi M, Sorribas V**. $Na^+$-independent phosphate transport in Caco2BBE cells. *Am J Physiol Cell Physiol*. 307: C1113-C1122, 2014.
9. **Candeal E, Caldas YA, Guillén N, Levi M, Sorribas V**. Intestinal phosphate absorption is mediated by multiple transport systems in rats. *Am J Physiol Gastrointest Liver Physiol*. 312: G355-G366, 2017.

10. **Couasnay G, Bon N, Devignes CS, Sourice S, Bianchi A, Véziers J, Weiss P, Elefteriou F, Provot S, Guicheux J, Beck-Cormier S, Beck L.** PiT1/Slc20a1 is required for endoplasmic reticulum homeostasis, chondrocyte survival, and skeletal development. *J Bone Miner Res.* 34: 387-398, 2019.
11. **Crouthamel MH, Lau WL, Leaf EM, Chavkin NW, Wallingford MC, Peterson DF, Li X, Liu Y, Chin MT, Levi M, Giachelli CM.** Sodium-dependent phosphate cotransporters and phosphate-induced calcification of vascular smooth muscle cells: redundant roles for PiT-1 and PiT-2. *Arterioscler Thromb Vasc Biol.* 33: 2625-2632, 2013.
12. **Dallaire L, Béliveau R**. Phosphate transport by capillaries of the blood-brain barrier. *J Biol Chem.* 267: 22323-22327, 1992.
13. **Forster IC, Loo DD, Eskandari S.** Stoichiometry and Na+ binding cooperativity of rat and flounder renal type II Na+–Pi cotransporters. *Am J Physiol.* 276: F644–649, 1999.
14. **Forster IC, Hernando N, Biber J, Murer H.** Phosphate transporters of the SLC20 and SLC34 families. *Mol Aspects Med.*34: 386-395, 2013.
15. **Giachelli CM.** The emerging role of phosphate in vascular calcification. *Kidney Int.* 75: 890-897, 2009.
16. **Giovannini D, Touhami J, Charnet P, Sitbon M, Battini JL.** Inorganic phosphate export by the retrovirus receptor XPR1 in metazoans. *Cell Rep*. 3: 1866-1873, 2013.
17. **Guillén N, Caldas YA, Levi M, Sorribas V**. Identification and expression analysis of type II and type III Pi transporters in the opossum kidney cell line. *Exp Physiol.* 104: 149-161, 2019.
18. **Ho AM, Johnson MD, Kingsley DM.** Role of the mouse ank gene in control of tissue calcification and arthritis. *Science.* 289:265-270, 2000.

19. **Hortells L, Sosa C, Millán Á, Sorribas V.** Critical parameters of the in vitro method of vascular smooth muscle cell calcification. *PLoS One*. 10: e0141751, 2015.
20. **Hortells L, Sosa C, Guillén N, Lucea S, Millán Á, Sorribas V.** Identifying early pathogenic events during vascular calcification in uremic rats. *Kidney Int*. 92: 1384-1394, 2017.
21. **Li X, Yang HY, Giachelli CM.** Role of the sodium-dependent phosphate cotransporter, Pit-1, in vascular smooth muscle cell calcification. *Circ Res.* 98: 905-912, 2006.
22. **Myint S, Butterworth PJ.** Phosphate transport across the basolateral membrane of chick kidney proximal tubule cells. *Cell Biochem Funct*. 7: 43-49, 1989.
23. **Prosdocimo DA, Douglas DC, Romani AM, O'Neill WC, Dubyak GR.** Autocrine ATP release coupled to extracellular pyrophosphate accumulation in vascular smooth muscle cells. *Am J Physiol Cell Physiol.* 296: C828-C839, 2009,
24. **Ravera S, Virkki LV, Murer H, Forster, IC.** Deciphering PiT transport kinetics and substrate specificity using electrophysiology and flux measurements. *Am J Physiol Cell Physiol.* 293: C606-C620, 2007.
25. **Romero MF, Chen AP, Parker MD, Boron WF.** The SLC4 family of bicarbonate ($HCO_3^-$) transporters. *Mol Aspects Med.* 34: 159-182, 2013.
26. **Salaün C, Leroy C, Rousseau A, Boitez V, Beck L, Friedlander G**. Identification of a novel transport-independent function of PiT1/SLC20A1 in the regulation of TNF-induced apoptosis. *J Biol Chem.* 285: 34408-34418, 2010.
27. **Segawa H, Kaneko I, Takahashi A, Kuwahata M, Ito M, Ohkido I, Tatsumi S, Miyamoto K**. Growth-related renal type II Na/Pi cotransporter. *J Biol Chem*. 277: 19665-19672, 2002.
28. **Solomon DH, Wilkins RJ, Meredith D, Browning JA.** Characterisation of inorganic phosphate transport in bovine articular chondrocytes. *Cell Physiol Biochem.* 20: 99-108, 2007.

29. **Sorribas V.** Slc20. **Encyclopedia of Signaling Molecules**, edited by Choi S: Springer, 2018, p. 4987–4994.
30. **Sorribas V, Guillén N, Sosa C.** Substrates and inhibitors of phosphate transporters: from experimental tools to pathophysiological relevance. P*flugers Arch.* 47: 53-65, 2019.
31. **Szczepanska-Konkel M, Yusufi AN, VanScoy M, Webster SK, Dousa TP**. Phosphonocarboxylic acids as specific inhibitors of Na+-dependent transport of phosphate across renal brush border membrane. *J Biol Chem*. 261:6375-6383, 1986.
32. **Villa-Bellosta R, Bogaert YE, Levi M, Sorribas V.** Characterization of phosphate transport in rat vascular smooth muscle cells: implications for vascular calcification. *Arterioscler Thromb Vasc Biol.* 2007;27:1030-1036.
33. **Villa-Bellosta R, Levi M, Sorribas V**. Vascular smooth muscle cell calcification and SLC20 inorganic phosphate transporters: effects of PDGF, TNF-alpha, and Pi. *Pflugers Arch*. 458: 1151-1161, 2009.
34. **Villa-Bellosta R, Sorribas V.** Different effects of arsenate and phosphonoformate on P(i) transport adaptation in opossum kidney cells. *Am J Physiol Cell Physiol.* 297: C516-C525, 2009.
35. **Villa-Bellosta R, Sorribas V.** Phosphonoformic acid prevents vascular smooth muscle cell calcification by inhibiting calcium-phosphate deposition. *Arterioscler Thromb Vasc Biol*. 29: 761-766, 2009.
36. **Villa-Bellosta R, Millan A, Sorribas V.** Role of calcium-phosphate deposition in vascular smooth muscle cell calcification. *Am J Physiol Cell Physiol*. 300: C210-C220, 2011.

## Figures

**Figure 1. Characteristics of Pi transport in confluent VSMC.** A. Total uptakes of Pi at increasing concentrations of substrate, in the presence or absence of sodium. The equation fitted to data includes an unsaturable component. Non-visible error bars are smaller than the symbols. B. Theoretical sodium-dependent and sodium-independent (choline chloride) transport components of total Pi uptake, according to the results of panel A. C. Effect of pH in the presence (white bars) and absence (black bars) of sodium. In A and C, every symbol and bar are the means of six data.

**Figure 2. Effect of confluence on VSMC.** A. Effect on total sodium-dependent and sodium-independent Pi uptakes as a function of tissue culture confluence. Symbols are the mean of 3 experimental values. B. Expression of the indicated RNAs in VSMC at 50% (black bars) and 100% (white bars) confluence. Bars show the means of three data. C. Protein expression of the corresponding RNAs analyzed in B and expressed in relation to ß-actin. Representative Western blots of target proteins are shown at the right. When more than one band is present, the specific signal is shown with an arrowhead. All western blots were normalized to ß-Actin, which was unchanged between samples on all blots showing no errors in loading. Full length images of all target genes and ß-Actin for all blots were provided during peer review. Only representative blots of target genes are shown for brevity. In B and C, asterisks mean significant differences with a t-test ($p < 0.05$). Bars are the means of 3 to 6 values.

**Figure 3. Role of chloride in Pi uptake and P efflux.** A. Effect of chloride on sodium-dependent and sodium-independent Pi uptakes under initial velocity conditions (only influx). *, $p < 0.05$ with a t-test. B. Phosphorus content in cell after 3 hours of incubation

639 with $^{32}$Pi in the presence or absence of chloride for the experiment shown in C and D. The
640 remaining P content after 2 hours of P exit is also shown, in the presence or absence of
641 chloride. The molecular entity of this phosphorus is unknown, and therefore only the mass
642 of P is considered. C. P released from cells after 3 hours of loading with 0.05 mM $^{32}$Pi.
643 $^{32}$Phosphorus was determined in uptake media at the indicated times, with the total P
644 expressed per milligram of VSMC protein. The slopes and the $r^2$ are shown for this
645 representative experiment. Both regression lines were significantly different. The 95%
646 confidence intervals of both linear regressions are also shown with two dashed confidence
647 bands. D. P exit per unit of time at every time point. Non-regression lines of exponential
648 decay curves are shown to help understand the P exit behavior. The calculated half-life
649 parameters and the decay rate constants are also shown. Inset: net P content in uptake
650 medium at every time point. In all four panels, the number of data per bar or symbol is six.

651 **Figure 4. Inhibition profile of Pi transport.** A. Effect of the indicated inhibitors on
652 sodium-dependent and sodium-independent Pi transport. Asterisks indicate significant
653 difference with respect to the Control condition, with an ANOVA and a Tukey post-test ($p <$
654 0.05). Pi (as inhibitor), sulfate, bicarbonate, arsenate, and PFA were used at 5 mM, oxalate
655 at 10 mM, and DIDS/SITS at 0.1 mM. Bars are the mean of 12 experimental data. B.
656 Microphotographs of VSMC after incubation in uptake solution, with or without calcium
657 for 10 minutes. Bar, 50 μm. C. No effect of DIDS and SITS on Pi transport resulting from
658 the expression of rat PiT1 and PiT2 in *Xenopus laevis* oocytes. Bars are the mean of 10
659 experimental data.

660 **Figure 5. Dose-response relationships.** The assays were performed at a constant Pi
661 concentration (0.05 mM Pi), while increasing the concentrations of inhibitors. Sulfate,

662 bicarbonate, and arsenate were assayed for dose-responses of sodium-independent Pi
663 transport, and DIDS/SITS were assayed for uptake in the presence of sodium chloride.
664 Figures show representative experiments of the inhibition assays, each of which was
665 performed three times. Every symbol represents the mean of triplicates.

666 **Figure 6. Determination of Ki values.** Michaelis-Menten saturation kinetics were
667 performed for sulfate in the absence of sodium (A) and for SITS in the presence of sodium
668 (B). For each saturation experiment a different concentration of inhibitors was used, as
669 indicated in the legends. Left, Lineweaver-Burk linear regressions. Right, non-linear
670 regression fits of a Michaelis-Menten equation to data, plus an unsaturable component.
671 Apparent affinities are indicated in the symbol legends. Every symbol represents the mean
672 of triplicates.

673 **Figure 7. Expression of anion exchangers.** A. Quantitative, real-time PCR of the
674 indicated anion exchanger RNAs from VSMC cultivated at 50% or 100% confluence. The
675 significance of different expressions was determined with a t-test. B. Resulting RNA
676 abundance inhibition after treatments with either scrambled or specific siRNAs after 48
677 hours. C. The resulting Pi transport after anion exchanger RNA interference 48 hours post-
678 transfection, in the presence or absence of sodium. Bars of panels A and B are the means of
679 triplicates. Bars of panel C show the means of 6 experimental data.

680 **Figure 8. Effect of VSMC incubation at a high Pi concentration.** A. No effect on Pi
681 uptake after 7 days of incubation with either 1 or 2 mM Pi. Bars show means of triplicates.
682 B. No effect on P exit from the cell after 2 hours of incubation with $^{32}P$. The graph
683 represents the accumulation of $^{32}P$ as grams of total phosphorus in uptake medium per
684 milligram of VSMC protein. Symbols show the means of six experimental data.

**Figure 9. Drawing depicting the Pi transport systems in VSMC.** Inward Pi transporters are shown at the left, including the known Slc20 members PiT1 and PiT2. Another sodium-dependent Pi transporter that is sensitive to stilbene-derivatives is also shown. Pi uptake systems also include a sodium-independent pathway (shown in the middle of the drawing), which handles both monobasic and dibasic phosphates, and it is weakly inhibited by sulfate. The transport system is most likely coupled to the exit of anions. Finally, the exit of Pi from the cell is partially coupled to the entrance of chloride, and it is resistant to DIDS and SITS.

# Figure 1

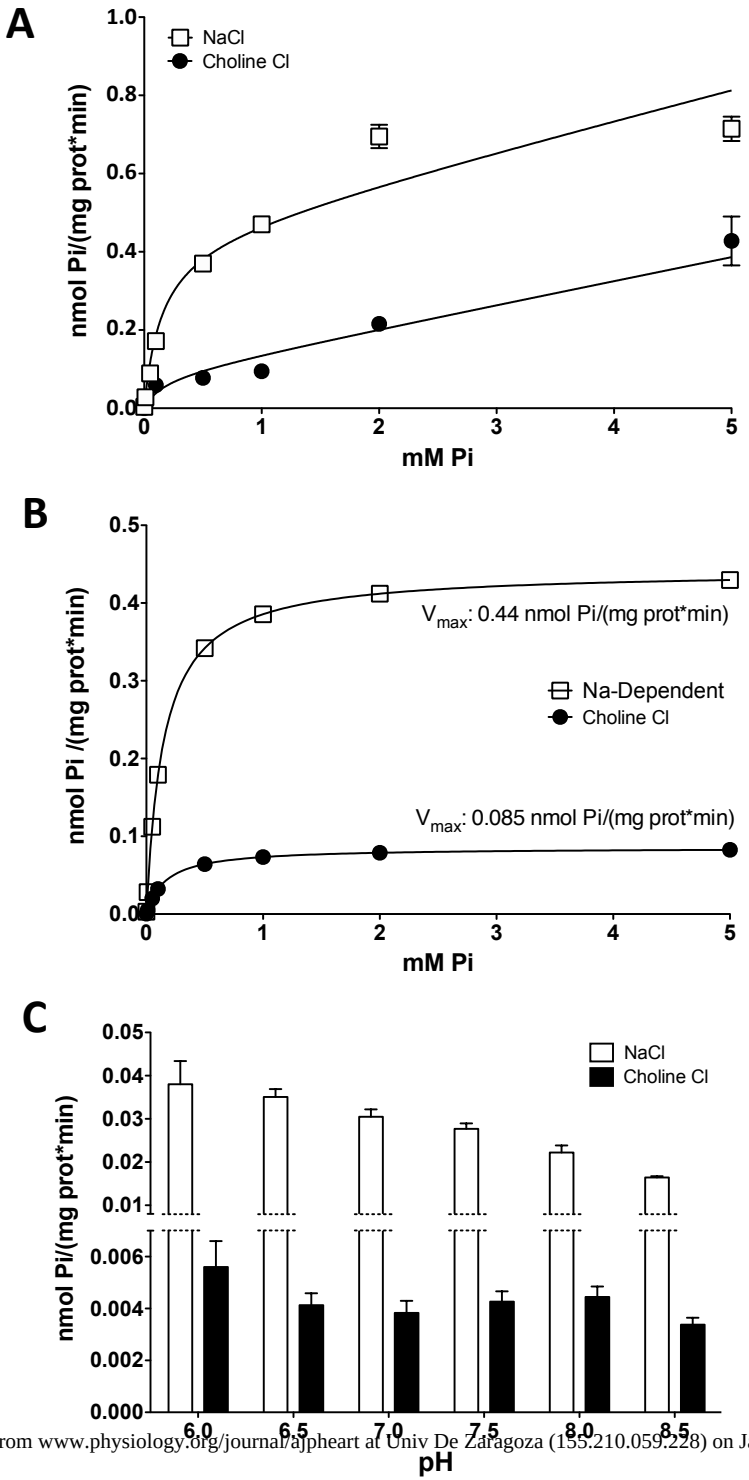

# Figure 2

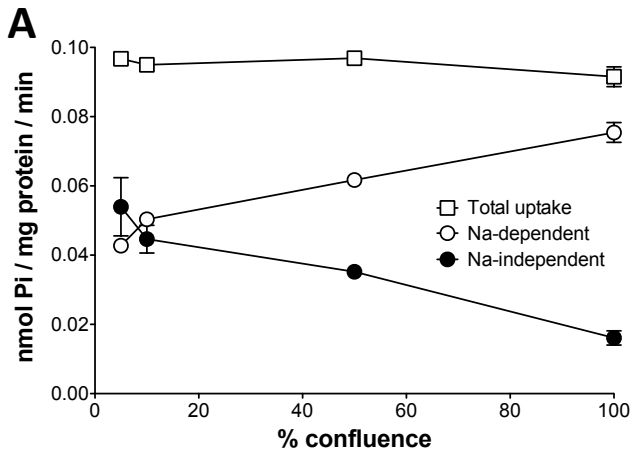


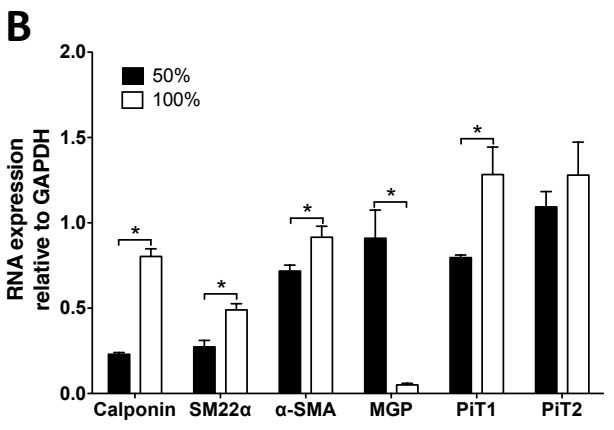


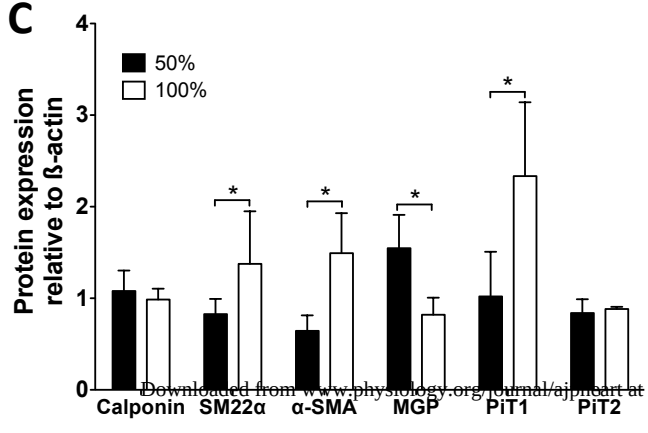


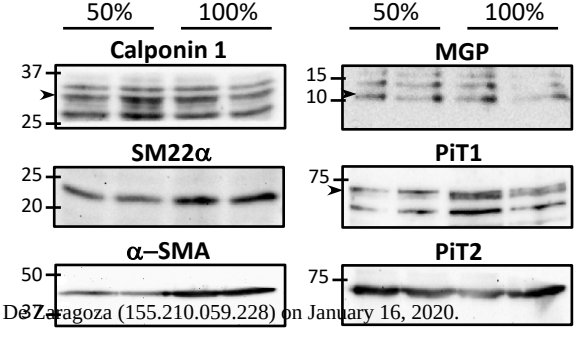

# Figure 3

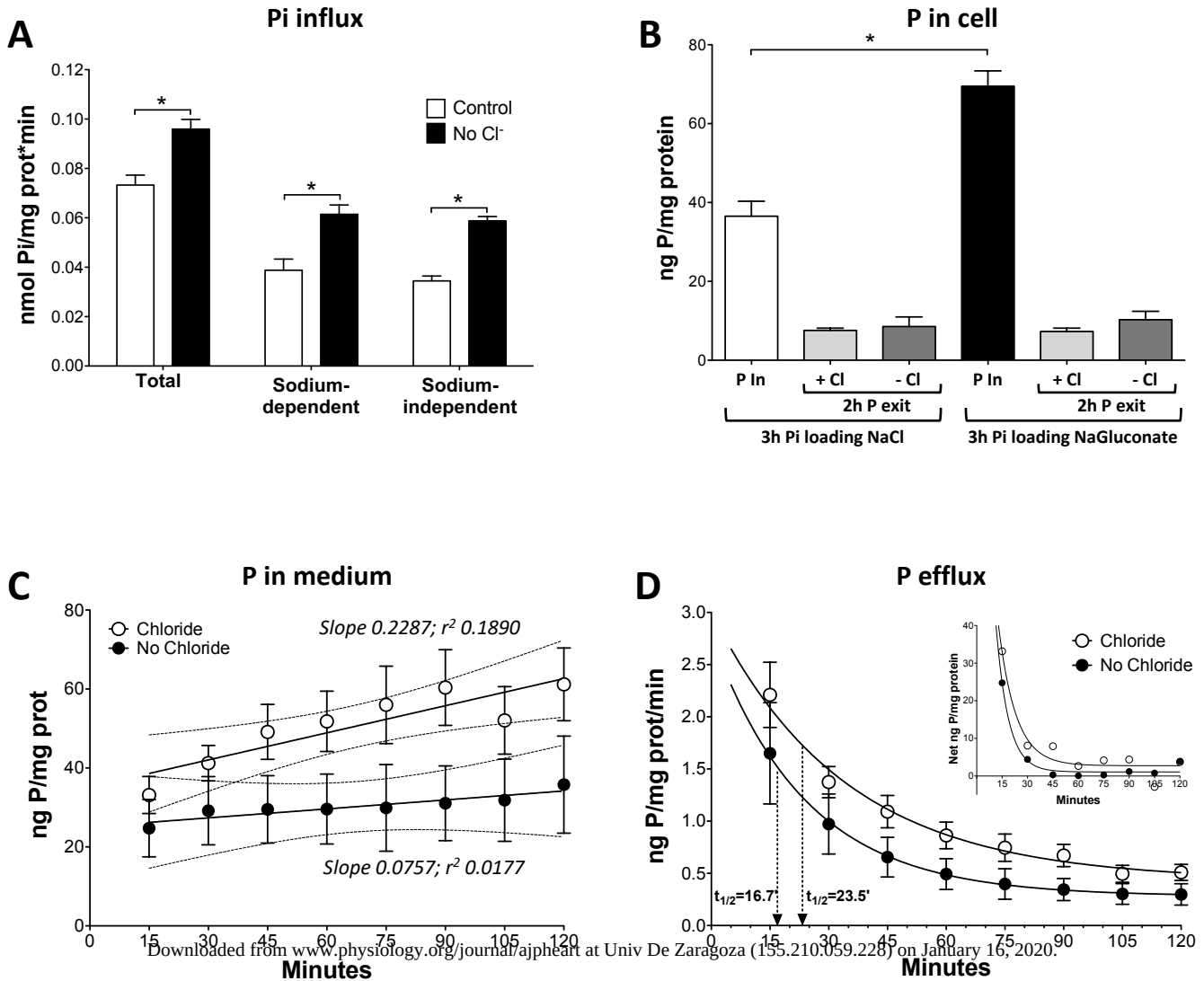

# Figure 4

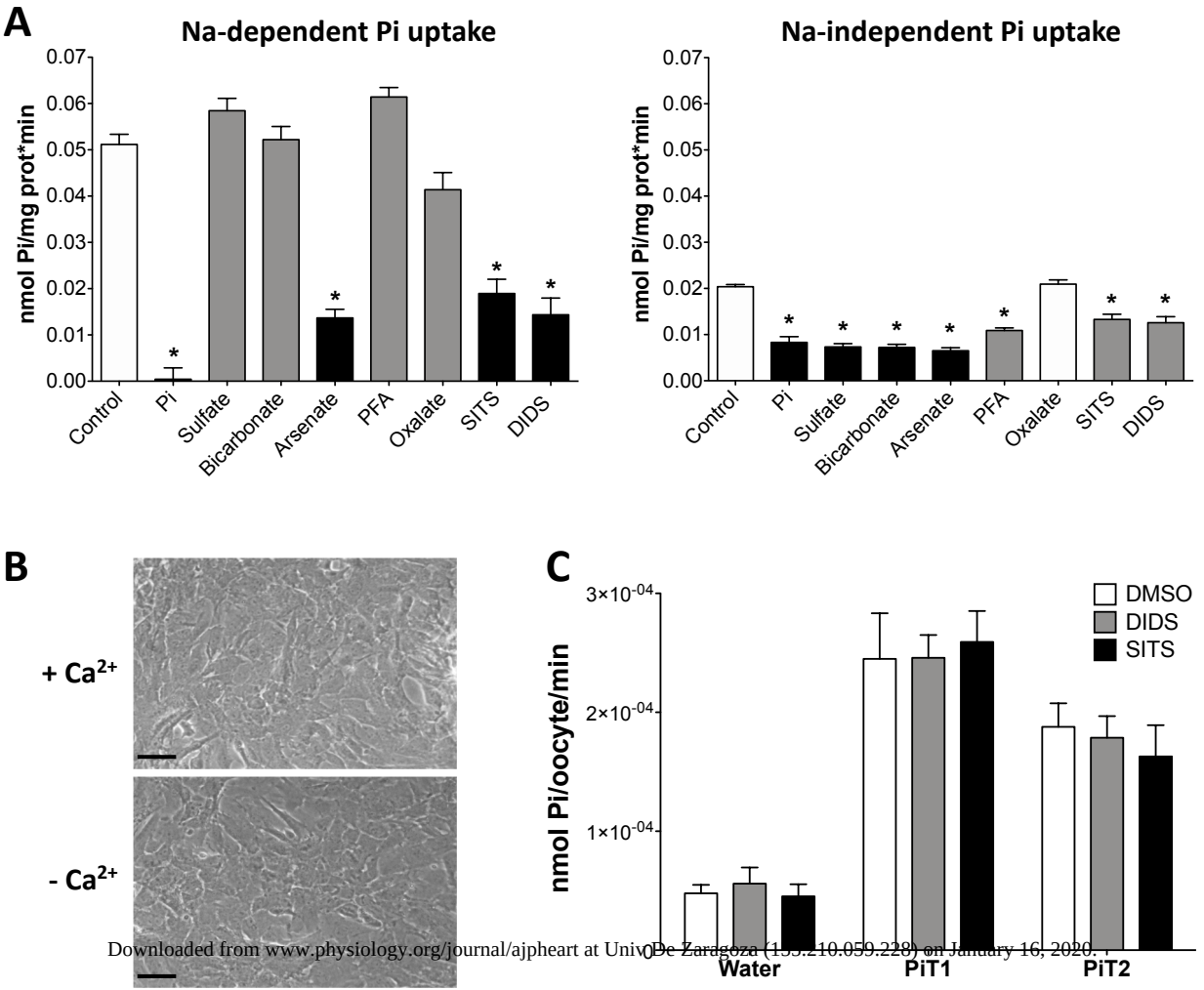

# Figure 5

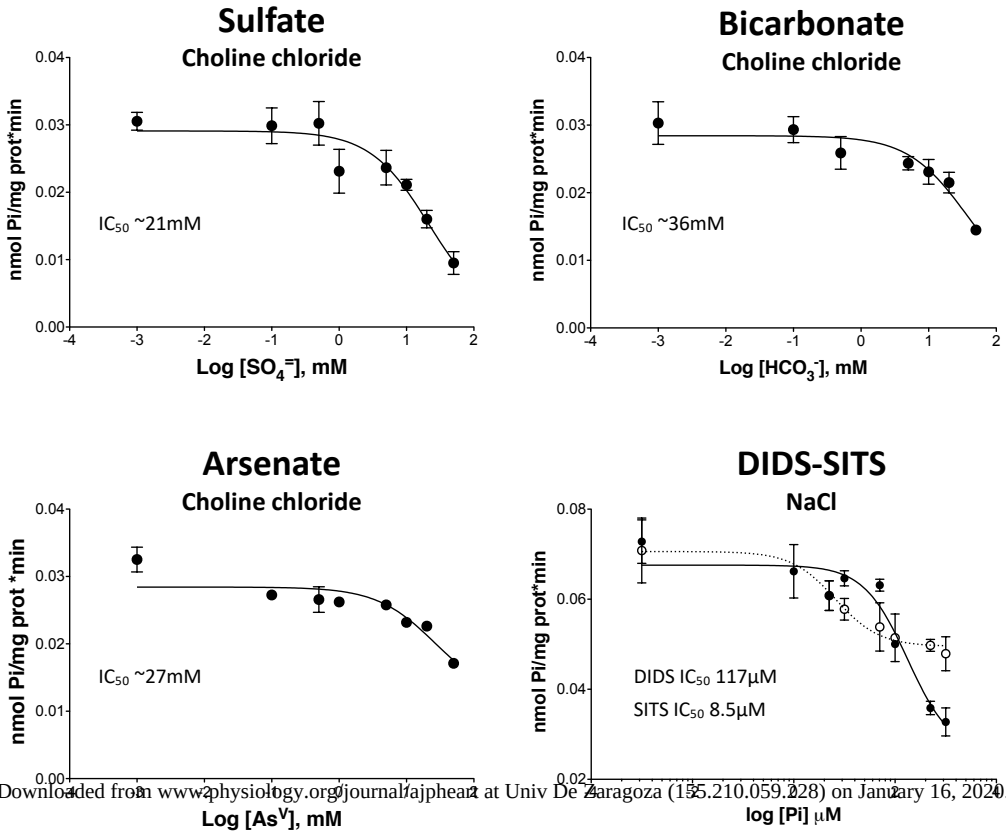

# Figure 6

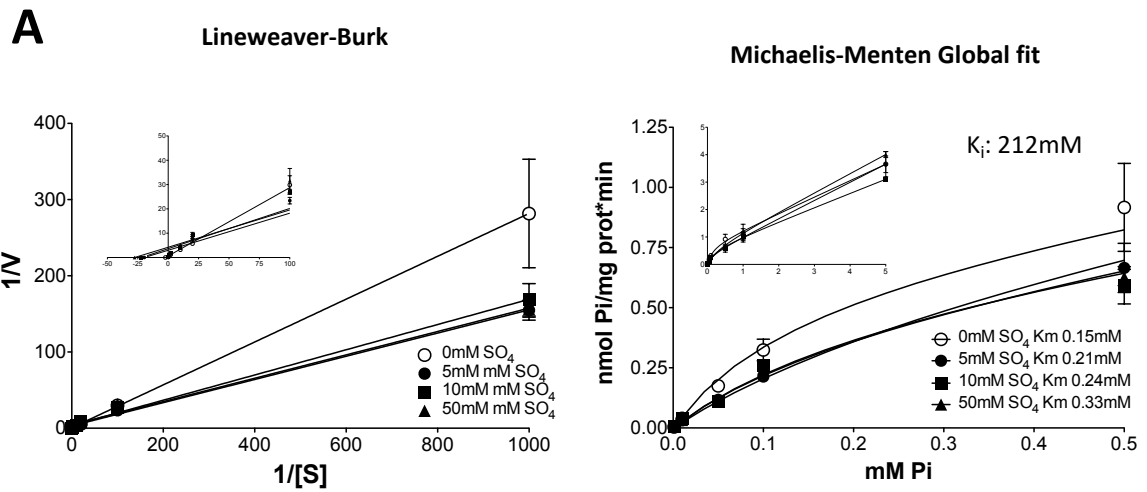


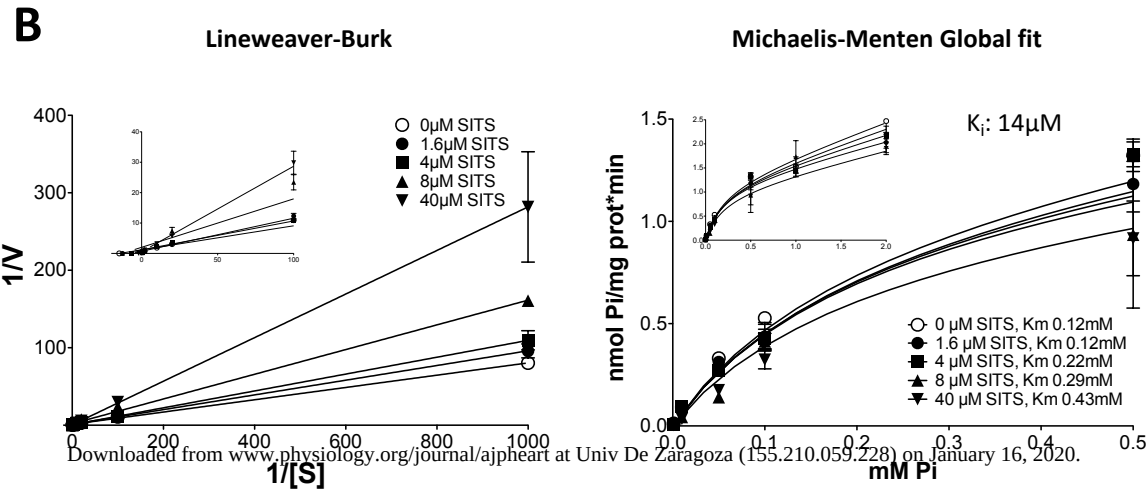

# Figure 7

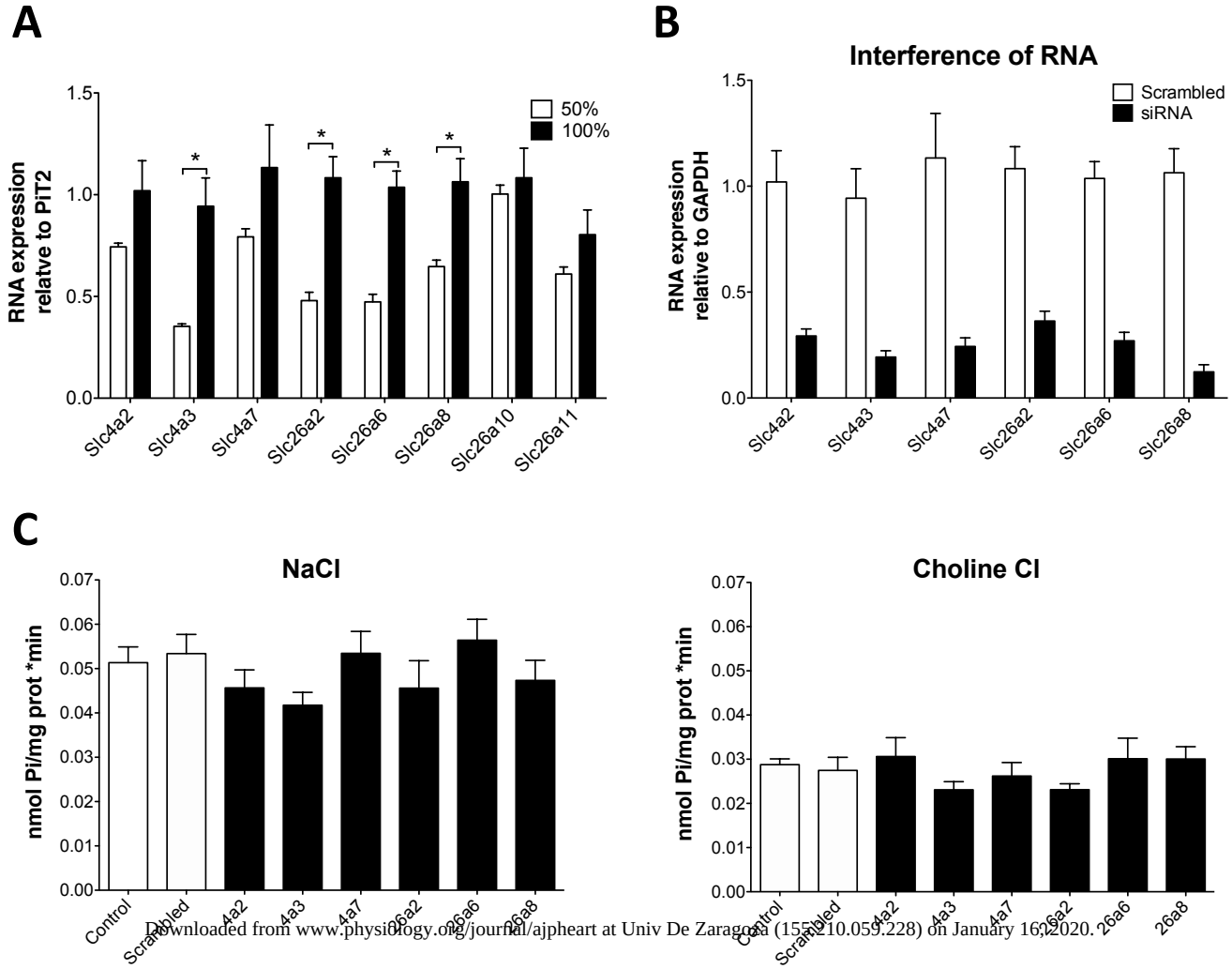

# Figure 8

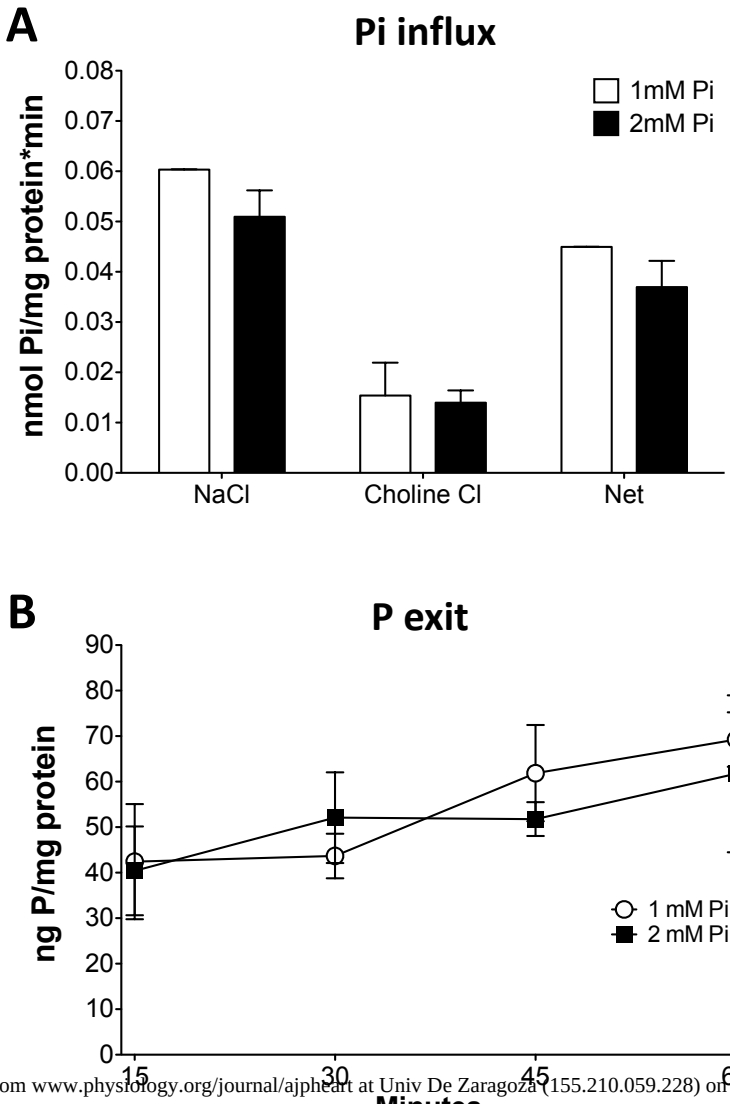

# Figure 9

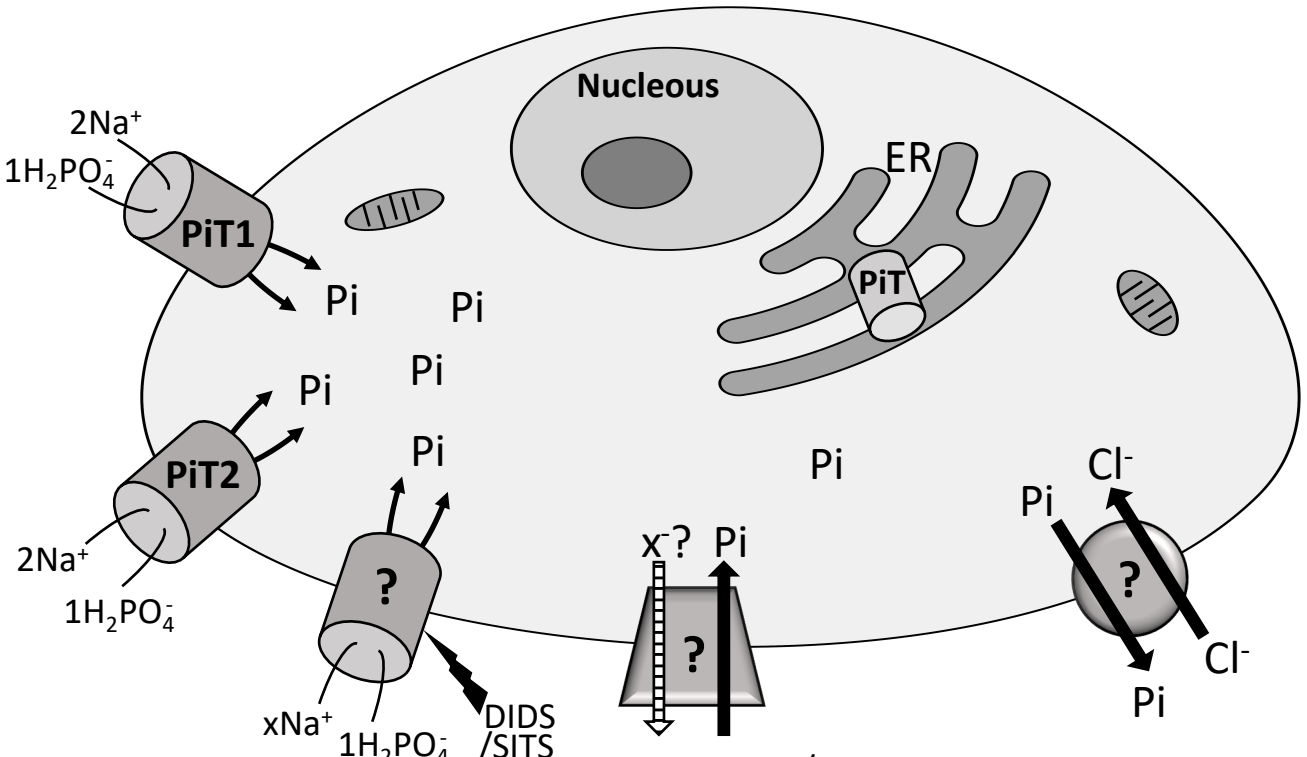

## Table 1. List of primers used for PCR

In real time PCR:

| Gene name | Accession number | Sense primer | Antisense primer |
|---|---|---|---|
| Calponin | D14437.1 | TCCGCACACTTTAACCGAG | ATCCATGAAGTTGCTCCCG |
| SM22α | NM_031549.2 | CAGACTGTTGACCTCTTTGAAG | TCTTATGCTCCTGGGCTTTC |
| α-SMA | BC158550.1 | CATCACCAACTGGGACGACA | TCCGTTAGCAAGGTCGGATG |
| MGP | NM_012862.1 | AACACCTTTATATCCCCTCAGC | GCGTTGTACCCGTAGATCAG |
| PiT1 | NM_031148.1 | CCGTCAGCAACCAGATCAACTC | CCCATGCAGTCTCCCACCTTG |
| PiT2 | NM_017223.2 | CTATTCCAAGAAGAGGCTCCG | TCAGGATCGGTCAGCTCAG |
| Slc4a2 | NM_017048.2 | TACCCGCACTACCTGAGTGA | CAAAAGTGATGGCAGGCGAC |
| Slc4a3 | NM_017049.1 | TGGGTCCAGATGTAGAAGAGGA | GCCGGTGAAACTCAAAGTCG |
| Slc4a7 | NM_058211 | GGCAAGAAACATTCTGACCCT | GGAAAGGTTTGAGGCAGACAG |
| Slc26a2 | NM_057127 | CTCATTGTCGTTGTGGCAGC | GGCATAAACCCGGTGGGAAT |
| Sc26a6 | NM_001143817.1 | AGCTAGAGGATCTGGGGCAC | ATATCGGGGTAACCAGCCCA |
| Slc26a8 | XM_008772779.1 | AGCTCTTCCCAAAGCGAACT | GGGAACTCGATGGGATAGCG |
| Slc26a10 | NM_001134595.2 | GCTCAGTGTAATGACTTGGTGC | TTCGGGCCAGTAGGTTTCAG |
| Slc26a11 | XM_006220967 | AGGAGGCTCTGGCTTGTTCA | AGTTTACCAGAGTGCCACAGC |

In non-quantitative PCR:

| Gene name | Accession number | Sense primer | Antisense primer |
|---|---|---|---|
| Slc26a1 | NM_022287.2 | GTACCTCCCGCCACGTTAAT | TCAGCCAAGTGTGGATCACC |
| Slc26a2 | NM_057127.1 | GGGGGCTCAAAGAGGATCAA | CGGTCAACTACCTCACCAATCA |
| Slc26a3 | NM_053755.2 | GCAGCAAGTGTGGCATTTCA | GAGGCTGTGGAGGCTGATTT |
| Slc26a4 | NM_019214.1 | CCTTTGGTTGGCGGATTCAC | CACAGACGGCAGTACAGGAG |
| Slc26a5 | NM_030840.1 | GCTGCACGTCAAGGACAAAG | ACCCTTAACGCATCTCTGGC |
| Slc26a6 | NM_001143817.1 | CTGTGCAAGTCCTCGTCTCC | AGTGAGATGGCAATGGCGAA |
| Slc26a7 | NM_001106638.1 | TGAGAAATGACGGGGGCAAA | TCTCTGCAGCTCAAACTCCG |
| Slc26a8 | XM_003753467.3 | GCTTAGCACAGAGCAGATCCA | GGTCCAGGTCAAACTCCAAGT |
| Slc26a9 | NM_001107172.1 | CTTCTCCCTGGCAATAGTGGG | GGGTCTGGAAGATCACAACCA |
| Slc26a10 | NM_001107172.1 | CCAGGATACTGGCTGACTCAC | GACCATCCACACGGCAAAGT |
| Slc26a11, v. I, II, IV | XM_006220967.2<br>XM_006220968.2<br>XM_006220967.2 | CCTCCTCCCCATCCTGAGAT | GTGACCGGGTAAGACGAGAC |
| Slc26a11, v. III | XM_001081843.4 | CTGAATCAATACTCCTCCTAGGGC | GTAAGGCTGAGTCCCTGGTTC |
| Slc4a1 | NM_012651.2 | AGATTTTCCAGGACTACCCGC | AGGATGAAGACAAGCAGAGCG |
| Slc4a2 | NM_017048.2 | AGCTGATCATGTCCACAGCG | TGGTTGCTGCCCAAGTCATA |
| Slc4a3 | NM_017049.1 | AGAAGATCCCTGAGGACGCT | TCCACTTTGGTCTGTTCCCG |
| Slc4a7 | NM_058211.2 | AGGTGGATTTCTTGGAGAGACC | CGTGGTGATCAGCCTCCTTAG |